

Improving complex shear modulus imaging quality through enhanced frequency combination techniques

Cuong-Thai Nguyen¹, Pham Thi Thu Ha², Pham Duy Phong², Quang Hai Luong³, Bao Bo Quoc¹, Duc-Tan Tran⁴

¹Faculty of Electronics Engineering, Hanoi University of Industry, Hanoi, Vietnam

²Faculty of Electronics and Telecommunication, Electric Power University, Hanoi, Vietnam

³Department of Biomedical Engineering, Faculty of Control Engineering, Le Quy Don Technical University, Hanoi, Vietnam

⁴Department of Electronics and Telecommunication, Faculty of Electrical and Electronic Engineering (FEEE), Phenikaa University, Hanoi, Vietnam

Article Info

Article history:

Received month dd, yyyy

Revised month dd, yyyy

Accepted month dd, yyyy

Keywords:

Complex shear modulus

Dual-frequency

Elastography

Imaging

Shear wave

ABSTRACT

This study aims to improve the accuracy of complex shear modulus imaging (CSMI), a technique used to assess the elasticity and viscosity of soft tissues, essential for analyzing tissue structure and detecting tumors. CSMI methods are primarily divided into quasi-static and dynamic approaches, with the dynamic method estimating the complex shear modulus (CSM) by combining particle velocity measurements with force excitation. However, CSM estimation is vulnerable to errors from noise and the estimation method itself. To address noise, various filtering techniques are commonly applied. Additionally, errors from the estimation process can be minimized using approaches like frequency combination methods. In this research, we introduce an enhanced frequency combination method that substantially increases the accuracy of CSM parameter estimation, leading to higher-quality CSMI outcomes. The proposed method achieves the lowest estimation error and the highest Q-index value compared to previous works. The proposed approach offers a valuable advancement in soft tissue imaging, supporting more reliable and precise diagnostic capabilities.

This is an open access article under the [CC BY-SA](https://creativecommons.org/licenses/by-sa/4.0/) license.



Corresponding Author:

Bao Bo Quoc

Faculty of Electronics Engineering, Hanoi University of Industry

No 298 Cau Dien Street, Bac Tu Liem District, Hanoi, Vietnam

Email: baobq@hau.edu.vn

1. INTRODUCTION

The assessment of soft tissue elasticity and viscosity is crucial for diagnosing and understanding various medical conditions, such as liver fibrosis and tumors. complex shear modulus imaging (CSMI) offers a method to quantify these mechanical properties, improving the diagnostic quality of tissue structure imaging. However, two main sources of error exist in estimating the complex shear modulus (CSM): noise and the limitations of the estimation methods. Although various filtering techniques address noise, improving the accuracy of CSM estimation methods-particularly with frequency combination techniques-remains a significant challenge. Current single-frequency methods do not optimally leverage the propagation characteristics of shear waves at different frequencies, which hinders precise measurement across different spatial regions within the tissue.

Several studies have contributed to the development of CSMI and elastography. In the beginning, shear wave elastography imaging (SWEI) was used to provide additional medical diagnosis data [1]–[12]. Afterwards, Youk *et al.* [13] reported that SWEI offers notable benefits over alternative imaging modalities

in terms of quantitative imaging and tissue elasticity contrast. Ferraioli *et al.* [14] demonstrated the use of shear waves in elastography to evaluate liver disease stages in 2014. SWEI equipment is now sold commercially. Nevertheless, it is uncommon to find equipment that can image both viscosity and elasticity.

To ascertain the qualities of these tissues, it is necessary to estimate the shear wave propagation velocity in tissues at one or more frequencies. This can be accomplished in a number of methods, including deep vibration as a mechanical force, surface vibration, and sonic radiation [15]–[19]. Huy *et al.* [20] used a vibrating needle to obtain the shear wave propagation, according to. One method to compute the CSM directly is to apply the Helmholtz algebra inversion transformation [12].

Despite advancements, several issues persist, particularly in improving the accuracy of CSM estimation at varying distances from the excitation source. High-frequency waves can accurately measure mechanical properties near the excitation source but suffer from attenuation in more distant regions. Conversely, low-frequency waves offer better accuracy in distant regions but lack precision near the source. Current methods fail to balance these trade-offs, leading to suboptimal CSMI results, especially in heterogeneous tissue environments. This manuscript addresses the gap by developing a dual-frequency combination method that adjusts for varying spatial distances.

This work introduces a novel approach to CSM estimation by combining data from two activation frequencies (100 Hz and 150 Hz) to enhance imaging quality and accuracy. The proposed method identifies a spatial threshold that allows for optimal use of low-frequency data in distant regions and high-frequency data near the excitation source. This spatially adaptive frequency combination technique minimizes errors, providing improved 2D reconstructions of elasticity and viscosity across tissue regions. Unlike previous methods that either relied on single frequencies or non-optimized frequency combinations, this method integrates both effectively, reducing CSM estimation errors in both near and far-field areas.

The subsequent sections describe the method and experimental setup in detail. The method section outlines the technical implementation of the frequency combination technique, including the mathematical models and simulation parameters. The results section presents an analysis of the performance improvements, showcasing the reduction in estimation errors and the enhanced image quality achieved with the dual-frequency method. Lastly, the discussion and conclusion sections evaluate the broader relevance of the proposed technique, emphasizing its potential applications in medical diagnostics and future research directions.

2. METHOD

This section outlines the experimental setup, procedures, and algorithms used to implement the dual-frequency combination method for CSMI. The approach is designed to improve estimation accuracy by leveraging both high and low-frequency data, and it is structured to allow replication of results. The method is grounded in theoretical models of shear wave propagation and experimentally validated using simulations of soft tissue environments. The following steps outline the key procedures used in the study.

2.1. Experimental setup

The experimental system consists of two main components: the excitation source and the imaging transducer [21]–[24]. A steel needle, acting as the excitation source, vibrates at two specific frequencies (100 Hz and 150 Hz) to generate shear waves that propagate through the tissue. The imaging transducer, typically an ultrasound probe, detects the movement of particles in the shear waves and calculates their velocity using Doppler technology in Figure 1. This setup mimics real-world tissue environments where shear waves interact differently at various distances from the excitation source.

The region of interest (ROI) is a two-dimensional (2D) tissue model, where the mechanical properties of soft tissue, such as elasticity and viscosity, are varied. A tumor is simulated within the tissue to reflect practical diagnostic scenarios. The transducer measures the shear wave velocity across the tissue, which provides information crucial for estimating the CSM.

2.2. Theoretical justification and novel approach

Standard single-frequency methods often struggle to accurately estimate mechanical properties across different spatial locations due to trade-offs between wave attenuation and propagation. High-frequency waves (150 Hz) provide better results near the needle, while low-frequency waves (100 Hz) perform better in distant regions. To address these challenges, this study proposes a novel dual-frequency combination method that optimally merges the data from both frequencies based on a spatial threshold.

According to the mathematical perspective, the CSM represents quantitative data regarding the characteristics of soft tissues as (1):

$$\mu = \alpha - i\omega\beta, \quad (1)$$

where the Kelvin-Voigt model calculates viscosity (β) and elasticity (α). Keep in mind that the needle is at $(0,0)$. $\omega=2\pi f$, f (Hz) is the excitation frequency, determines the value of μ . Accurate CSM estimation close to the needle is made possible by higher stimulation frequencies, which cause shear waves in the tissue to propagate more quickly. Higher frequencies, however, may also cause shear waves to propagate through the tissue with greater attenuation, which makes it more difficult to quantify stiffness precisely in areas that are farther away from the needle. Lower excitation frequencies cause waves to propagate more slowly yet improve estimating performance in far-off locations. As a result, the double-frequency stimulation method used in this work uses frequencies of 150 Hz and 100 Hz. Our algorithm is outlined in Figure 2.

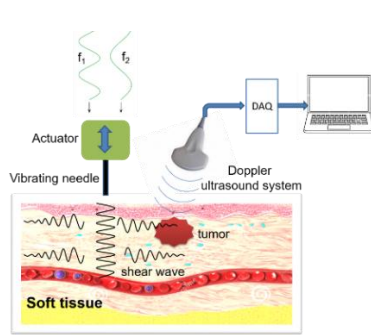


Figure 1. Data collection and excitation for the suggested shear wave estimating system

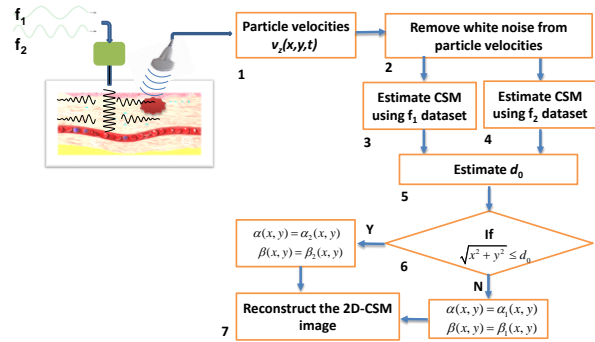


Figure 2. Proposed algorithm

When the needle, powered by an actuator running at a frequency of f_1 , can be represented by [25], the CSM is estimated.

$$\alpha_1(x, y) = R \left\{ \frac{-\lambda \omega_1^2 V_z(x, y, \omega_1)}{\nabla^2 V_z(x, y, \omega_1)} \right\} \quad (2)$$

and

$$\beta_1(x, y) = I \left\{ \frac{-\lambda \omega_1 V_z(x, y, \omega_1)}{\nabla^2 V_z(x, y, \omega_1)} \right\} \quad (3)$$

Likewise, using a higher frequency of $f_2=150$ Hz for the remaining excitation time resulted in:

$$\alpha_2(x, y) = R \left\{ \frac{-\lambda \omega_2^2 V_z(x, y, \omega_2)}{\nabla^2 V_z(x, y, \omega_2)} \right\} \quad (4)$$

and

$$\beta_2(x, y) = I \left\{ \frac{-\lambda \omega_2 V_z(x, y, \omega_2)}{\nabla^2 V_z(x, y, \omega_2)} \right\} \quad (5)$$

where $V_z(x, y, \omega_1)$ and $V_z(x, y, \omega_2)$ are Fourier transforms at ω_1 and ω_2 . The term $\nabla^2 V_z(x, y, \omega_1)$ denotes the Laplace operator of $V_z(x, y, \omega_1)$; and $\nabla^2 V_z(x, y, \omega_2)$ denotes the Laplace operator of $V_z(x, y, \omega_2)$.

As shown in Figure 2, setting up the simulation's required settings is the initial stage. Time intervals, frequencies, spatial locations, and other components of the simulation process will all be defined by these parameters. In the second step, the needle is vibrated at a frequency of 100 Hz from the start of the simulation ($t=0$) until 0.5 T. A key component of the modeling process is the needle's oscillation at this particular frequency. The needle vibrates once more in the third step, but at a frequency of 150 Hz this time (from 0.5 T to T). The measured particle velocities undergo noise removal to ensure cleaner signals for analysis. Subsequently, the cleaned velocities from the first and second excitation frequencies are used to estimate the CSM for each dataset. The third step involves estimating the CSM α_1 β_1 at each location using the f_1 dataset and Algorithm 1 ((2) and (3)). Similarly, in the fourth step, the focus is on estimating the CSM α_2 β_2 at each location using Algorithm 1 ((4) and (5)).

In step 5, we explore the estimated CSM (α_1 β_1) and (α_2 β_2) in order to find the optimal threshold d_0 as shown in Figure 2. The minimum value of d_0 is 0 (near the needle) and the maximum one is d_{\max} (end of the ROI). A *For-Loop* will be used to scan the value of d_0 in order to minimize the average of relative errors

in (6). This approach seeks to obtain accurate CSM estimation close to the needle as well as far from it by taking into account the trade-off between excitation frequency and wave propagation properties. Ultimately, the 2D-CSM image is reconstructed using the determined (α, β) values.

To assess how well the proposed method estimates 2D CSMs, an error parameter is given (6):

$$\epsilon_{\alpha} = \frac{1}{M \times N} \sum_{i=1}^M \sum_{j=1}^N \frac{\alpha_{i,j} - \hat{\alpha}_{i,j}}{\alpha_{i,j}},$$

$$\epsilon_{\beta} = \frac{1}{M \times N} \sum_{i=1}^M \sum_{j=1}^N \frac{\beta_{i,j} - \hat{\beta}_{i,j}}{\beta_{i,j}},$$
(6)

where ϵ_{α} and ϵ_{β} represent the normalized errors for the estimated 2D elasticity and viscosity fields, respectively. $M \times N$ is the total number of pixels in the image (image size). $\alpha_{i,j}$, and $\hat{\alpha}_{i,j}$ denote the ideal and estimated elasticity values at location (i, j) . Similarly, $\beta_{i,j}$ and $\hat{\beta}_{i,j}$ represent the ideal and estimated viscosity values.

Another way to assess performance is by using the universal image quality (Q) index. This metric quantifies image distortion by considering three key factors: correlation loss, changes in brightness (luminance distortion), and changes in contrast.

$$Q = \frac{4\sigma_{xy}\bar{x}\bar{y}}{(\sigma_x^2 + \sigma_y^2)[(\bar{x})^2 + (\bar{y})^2]}$$
(7)

where \bar{x} and \bar{y} are the mean of the original image and the reconstructed one, respectively; σ_x^2 and σ_y^2 are the variances of x and y ; and σ_{xy} is the covariance between x and y .

2.3. Validation and reproducibility

The experimental setup is validated through a series of simulations using a 120×120 mm tissue model in Figure 3. In our simulation a vibrating needle was positioned at the upper left corner of the tissue, as shown in Figure 3(a). Figure 3(a) also shows the elasticity images reconstructed using 100 Hz data; Figure 3(b) presents the images reconstructed using 150 Hz data; Figure 3(c) depicts the mixed-frequency reconstruction without applying the optimal threshold; and Figure 3(d) demonstrates the combined-frequency reconstruction with the optimal threshold.

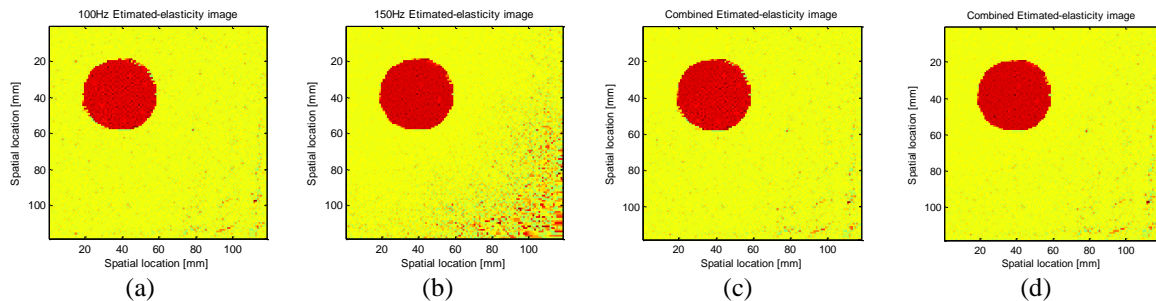


Figure 3. CSMI for four scenarios; (a) displays the elasticity pictures that were reconstructed using 100 Hz data, (b) displays the images that were reconstructed using 150 Hz data, (c) displays the mixed frequency reconstruction that did not use the ideal threshold, and (d) displays the combined frequency reconstruction with the optimal threshold d_0

The tumor itself had a radius of 20 mm. The elasticity of the surrounding tissue was set to be 6000 Pascals (Pa), with a viscosity of 1.2 Pascals-seconds (Pa·s). The tumor was slightly stiffer, with an elasticity of 9000 Pa and a viscosity of 1.8 Pa·s. The density of the entire tissue was set to 1000 kg/m³. The algorithm is applied to estimate the CSM and reconstruct 2D images of the tissue's mechanical properties. The results are compared with ideal values to verify the accuracy of the proposed method. The parameters and procedures outlined are designed to ensure that the experiment can be fully replicated. All steps, from data collection to image reconstruction, have been detailed to provide clarity for researchers attempting to confirm or extend the findings.

3. RESULTS AND DISCUSSION

We examined the shear wave particle velocity at uniformly spaced places within the tissue's 2D plane. These locations were spaced one millimeter apart in the X and Y axes, the horizontal and vertical

directions, respectively. Table 1 presents the investigation of the distance threshold to find the optimal threshold d_0 . The first row represent different distance thresholds, ranging from $d=50:10:110$. Three metrics are analyzed: ϵ_α (the normalized errors of elasticity using combined dataset), ϵ_α at 100 Hz (the normalized errors of elasticity using 100 Hz dataset), and ϵ_α at 150 Hz (the normalized errors of elasticity using 150 Hz dataset). The results indicate that there is an optimal threshold d_0 around 90 where the error is minimized. The optimal threshold d_0 of 90 is also obtained when analyzing of ϵ_β and Q .

Table 1. Investigation of the distance threshold to find the optimal threshold d_0

	d=110	d=100	d=90	d=80	d=70	d=60	d=50
ϵ_α	2.4661×10^{-4}	2.3116×10^{-4}	2.2541×10^{-4}	2.2576×10^{-4}	2.3000×10^{-4}	2.3597×10^{-4}	2.4097×10^{-4}
ϵ_α at 100 Hz	2.4845×10^{-4}	2.4845×10^{-4}	2.4845×10^{-4}	2.4845×10^{-4}	2.4845×10^{-4}	2.4845×10^{-4}	2.4845×10^{-4}
ϵ_α at 150 Hz	4.6557×10^{-4}	4.6557×10^{-4}	4.6557×10^{-4}	4.6557×10^{-4}	4.6557×10^{-4}	4.6557×10^{-4}	4.6557×10^{-4}

We first analyzed the recovered image using two individual datasets acquired at 100 Hz and 150 Hz. The 100 Hz data revealed superior image quality in the far needle region compared to the 150 Hz data. Conversely, the 150 Hz data provided better recovered image quality in the area near the needle. Therefore, combining the 150 Hz data near the needle with the 100 Hz data from the far region offers superior recovery results compared to using either dataset alone. This is confirmed in Figure 3(c). Furthermore, our proposed method for finding the optimal threshold to combine these datasets yields the best results, as demonstrated in Figure 3(d).

Table 2 summarizes the performance of the proposed method compared to other approaches. It shows that the proposed method achieves the lowest estimation error. This means it produces results closest to the actual values, compared to methods using a single frequency or combining multiple frequencies without an optimal threshold. The suggested method also outperforms previous approaches in terms of Q-index value. The Q-index is a measure of image quality, so a higher value indicates that the proposed method produces images with less distortion.

Table 2. Metrics for assessing CSM estimates

	100 Hz	150 Hz	100 and 150 Hz data (without threshold)	100 and 150 Hz data (proposed method)
ϵ_α	2.4845×10^{-4}	4.6557×10^{-4}	2.4097×10^{-4}	2.2541×10^{-4}
ϵ_β	0.0017	0.0018	0.0016	0.0014
Q_α	0.4457	0.3734	0.4457	0.4514
Q_β	0.1710	0.2060	0.2063	0.2331

We offer some unique benefits that differentiate our approach from other approaches in the sector [26]–[31]. First and foremost, our method is unique in that it only requires two datasets to be obtained, each at different vibration frequencies (e.g., 100 Hz and 150 Hz). With this architecture, there is no need to fit multi-frequency data into a complicated viscoelastic medium rheological model [27]. As such, the data collection procedure is significantly simplified, departing from previous studies' methods, which frequently involved a painstaking concentration on particular frequency ranges for wave production and shear wave velocity dispersion measurements. Our data collection methodology's intrinsic simplicity facilitates experimentation and reduces error sources that may arise from more complex multi-frequency data fitting techniques.

As can be seen from the findings shown in Figures 3(b) and (d), combined-frequency reconstruction performs better than traditional single-frequency stimulation techniques. This improvement demonstrates how employing various frequencies during the reconstruction process can lead to greater accuracy in capturing tissue viscosity and elasticity as well as improved image quality. These results confirm the suggested combined-frequency technique's superiority over the conventional single-frequency approach.

Table 2 offers important new information on how well our suggested strategy works. In comparison to the single-frequency method and the combination one without optimal threshold, the suggested method yields the minimum estimation error, demonstrating higher accuracy in estimating the target parameters. Furthermore, when compared to competing methods, our suggested solution has a higher Q-index value, indicating better signal integrity and quality preservation. These outperform other methods in terms of performance.

4. CONCLUSION

This study proposes a novel frequency combination method to improve the accuracy of CSMI, which is vital for assessing the elasticity and viscosity of soft tissues. CSMI, used extensively in tissue structure research and tumor detection, operates through both quasi-static and dynamic techniques, with the

latter relying on particle velocity measurements and force excitation to estimate the CSM. Our proposed frequency combination method addresses these estimation errors effectively, thereby significantly improving the quality of CSM parameter estimation. The findings from this study suggest that incorporating this method can lead to more reliable and accurate CSMI, advancing its application in medical diagnostics and research. In the future work, we will investigate how the method can be integrated into clinical settings for real-time diagnosis and monitoring of tissue conditions.

FUNDING INFORMATION

This work was supported by the Hanoi University of Industry, Vietnam under Grand No. 12-2024-RD/HD-DHCN.

AUTHOR CONTRIBUTIONS STATEMENT

This journal uses the Contributor Roles Taxonomy (CRediT) to recognize individual author contributions, reduce authorship disputes, and facilitate collaboration.

Name of Author	C	M	So	Va	Fo	I	R	D	O	E	Vi	Su	P	Fu
Cuong-Thai Nguyen	✓		✓				✓			✓				✓
Pham Thi Thu Ha						✓			✓		✓			
Pham Duy Phong				✓	✓			✓	✓					
Quang Hai Luong		✓	✓				✓		✓					
Bao Bo Quoc	✓	✓			✓					✓			✓	✓
Duc-Tan Tran	✓		✓					✓		✓			✓	

C : Conceptualization

M : Methodology

So : Software

Va : Validation

Fo : Formal analysis

I : Investigation

R : Resources

D : Data Curation

O : Writing - Original Draft

E : Writing - Review & Editing

Vi : Visualization

Su : Supervision

P : Project administration

Fu : Funding acquisition

CONFLICT OF INTEREST STATEMENT

Authors state no conflict of interest.

INFORMED CONSENT

We have obtained informed consent from all individuals included in this study.

DATA AVAILABILITY

Data availability is not applicable to this paper as no new data were created or analyzed in this study.





REFERENCES

- [1] S. J. Kwon and M. K. Jeong, "Advances in ultrasound elasticity imaging," *Biomedical Engineering Letters*, vol. 7, no. 2, pp. 71–79, May 2017, doi: 10.1007/s13534-017-0014-7.
- [2] J. Ormachea and K. J. Parker, "Elastography imaging: the 30 year perspective," *Physics in Medicine & Biology*, vol. 65, no. 24, Nov. 2020, doi: 10.1088/1361-6560/abca00.
- [3] J.-L. Gennisson, T. Deffieux, M. Fink, and M. Tanter, "Ultrasound elastography: Principles and techniques," *Diagnostic and Interventional Imaging*, vol. 94, no. 5, pp. 487–495, May 2013, doi: 10.1016/j.diii.2013.01.022.
- [4] E. Budelli *et al.*, "A diffraction correction for storage and loss moduli imaging using radiation force based elastography," *Physics in Medicine and Biology*, vol. 62, no. 1, pp. 91–106, Jan. 2017, doi: 10.1088/1361-6560/62/1/91.
- [5] J. Marcon *et al.*, "Three-dimensional vs. two-dimensional shear-wave elastography of the testes—preliminary study on a healthy collective," *Clinical Hemorheology and Microcirculation*, vol. 64, no. 3, pp. 447–456, Jan. 2017, doi: 10.3233/CH-168115.
- [6] K. Skerl, S. Cochran, and A. Evans, "First step to facilitate long-term and multi-centre studies of shear wave elastography in solid breast lesions using a computer-assisted algorithm," *International Journal of Computer Assisted Radiology and Surgery*, vol. 12, no. 9, pp. 1533–1542, Sep. 2017, doi: 10.1007/s11548-017-1596-3.
- [7] Y. Wang *et al.*, "Three-dimensional Ultrasound Elasticity Imaging on an Automated Breast Volume Scanning System," *Ultrasonic Imaging*, vol. 39, no. 6, pp. 369–392, Nov. 2017, doi: 10.1177/0161734617712238.
- [8] A. Yamamoto *et al.*, "Shear wave velocity measurement of upper trapezius muscle by color Doppler shear wave imaging," *Journal of Medical Ultrasonics*, vol. 45, no. 1, pp. 129–136, Jan. 2018, doi: 10.1007/s10396-017-0803-8.
- [9] C. Zhang and Z. Zhang, "2D Ultrasonic Elastography Using Beam Steering and Iterative Correction," *Journal of Medical Imaging*




- and Health Informatics, vol. 7, no. 1, pp. 211–216, Feb. 2017, doi: 10.1166/jmihi.2017.2008.
- [10] C. J. Moore, M. D. M. Hossain, and C. M. Gallippi, “2D ARFI and Viscoelastic Response (VisR) anisotropy imaging in skeletal muscle,” in *2017 IEEE International Ultrasonics Symposium (IUS)*, Sep. 2017, pp. 1–4, doi: 10.1109/ULTSYM.2017.8091741.
- [11] C. Papadacci, E. A. Bunting, and E. E. Konofagou, “3D Quasi-Static Ultrasound Elastography With Plane Wave In Vivo,” *IEEE Transactions on Medical Imaging*, vol. 36, no. 2, pp. 357–365, Feb. 2017, doi: 10.1109/TMI.2016.2596706.
- [12] T. Q.-Huy, N. T. H. Yen, T. G. Le, and D.-T. Tran, “Two-dimensional viscoelastic imaging using an enhanced FDTD-AHI approach,” *Research on Biomedical Engineering*, vol. 37, no. 2, pp. 339–349, Jun. 2021, doi: 10.1007/s42600-021-00130-x.
- [13] J. H. Youk, H. M. Gweon, and E. J. Son, “Shear-wave elastography in breast ultrasonography: the state of the art,” *Ultrasonography*, vol. 36, no. 4, pp. 300–309, Oct. 2017, doi: 10.14366/usg.17024.
- [14] G. Ferraioli, P. Parekh, A. B. Levitov, and C. Filice, “Shear Wave Elastography for Evaluation of Liver Fibrosis,” *Journal of Ultrasound in Medicine*, vol. 33, no. 2, pp. 197–203, Feb. 2014, doi: 10.7863/ultra.33.2.197.
- [15] Y. Wang and M. F. Insana, “Viscoelastic Properties of Rodent Mammary Tumors Using Ultrasonic Shear-Wave Imaging,” *Ultrasonic Imaging*, vol. 35, no. 2, pp. 126–145, Apr. 2013, doi: 10.1177/0161734613477321.
- [16] Q. Wang, Y. Shi, F. Yang, and S. Yang, “Quantitative photoacoustic elasticity and viscosity imaging for cirrhosis detection,” *Applied Physics Letters*, vol. 112, no. 21, May 2018, doi: 10.1063/1.5021675.
- [17] R. Gerami *et al.*, “A literature review on the imaging methods for breast cancer,” *International Journal of Physiology, Pathophysiology and Pharmacology*, vol. 14, no. 3, pp. 171–176, 2022.
- [18] N. G. Ramião, P. S. Martins, R. Rynkevici, A. A. Fernandes, M. Barroso, and D. C. Santos, “Biomechanical properties of breast tissue, a state-of-the-art review,” *Biomechanics and Modeling in Mechanobiology*, vol. 15, no. 5, pp. 1307–1323, 2016, doi: 10.1007/s10237-016-0763-8.
- [19] C. C. Park *et al.*, “Magnetic Resonance Elastography vs Transient Elastography in Detection of Fibrosis and Noninvasive Measurement of Steatosis in Patients With Biopsy-Proven Nonalcoholic Fatty Liver Disease,” *Gastroenterology*, vol. 152, no. 3, pp. 598–607.e2, Feb. 2017, doi: 10.1053/j.gastro.2016.10.026.
- [20] T. Q.-Huy, P. T. Doan, N. T. H. Yen, and D.-T. Tran, “Shear wave imaging and classification using extended Kalman filter and decision tree algorithm,” *Mathematical Biosciences and Engineering*, vol. 18, no. 6, pp. 7631–7647, 2021, doi: 10.3934/mbe.2021378.
- [21] H. Zhang *et al.*, “Fluidity and elasticity form a concise set of viscoelastic biomarkers for breast cancer diagnosis based on Kelvin–Voigt fractional derivative modeling,” *Biomechanics and Modeling in Mechanobiology*, vol. 19, no. 6, pp. 2163–2177, Dec. 2020, doi: 10.1007/s10237-020-01330-7.
- [22] B. Qiang, J. C. Brigham, S. Aristizabal, J. F. Greenleaf, X. Zhang, and M. W. Urban, “Modeling transversely isotropic, viscoelastic, incompressible tissue-like materials with application in ultrasound shear wave elastography,” *Physics in Medicine and Biology*, vol. 60, no. 3, pp. 1289–1306, Feb. 2015, doi: 10.1088/0031-9155/60/3/1289.
- [23] F. L. Teixeira *et al.*, “Finite-difference time-domain methods,” *Nature Reviews Methods Primers*, vol. 3, no. 1, p. 75, Oct. 2023, doi: 10.1038/s43586-023-00257-4.
- [24] M. Bhatt *et al.*, “Reconstruction of Viscosity Maps in Ultrasound Shear Wave Elastography,” *IEEE Transactions on Ultrasonics, Ferroelectrics, and Frequency Control*, vol. 66, no. 6, pp. 1065–1078, Jun. 2019, doi: 10.1109/TUFFC.2019.2908550.
- [25] M. Belonosov, M. Dmitriev, V. Kostin, D. Neklyudov, and V. Tcheverda, “An iterative solver for the 3D Helmholtz equation,” *Journal of Computational Physics*, vol. 345, pp. 330–344, Sep. 2017, doi: 10.1016/j.jcp.2017.05.026.
- [26] Q. H. Luong, M. C. Nguyen, T. That-Long, and D. T. Tran, “Complex shear modulus estimation using integration of LMS/AHI algorithm,” *International Journal of Advanced Computer Science and Applications*, vol. 9, no. 8, pp. 584–589, 2018, doi: 10.14569/ijacsa.2018.090874.
- [27] Y. Yamakoshi, M. Ota, Z. Liu, S. Abe, and K. Taniuchi, “3-D observation of punctual needle by 2-D shear wave imaging under forced vibration of needle,” in *2018 IEEE International Ultrasonics Symposium (IUS)*, Oct. 2018, pp. 1–9, doi: 10.1109/ULTSYM.2018.8579937.
- [28] P. Kijanka and M. W. Urban, “Local Phase Velocity Based Imaging of Viscoelastic Phantoms and Tissues,” *IEEE Transactions on Ultrasonics, Ferroelectrics, and Frequency Control*, vol. 68, no. 3, pp. 389–405, Mar. 2021, doi: 10.1109/TUFFC.2020.2968147.
- [29] Y. Wang and M. F. Insana, “Wave propagation in viscoelastic materials,” in *Ultrasound Elastography for Biomedical Applications and Medicine*, 2016, pp. 118–127, doi: 10.1002/9781119021520.ch9.
- [30] E. Machado, S. E. Romero, G. Flores, and B. Castaneda, “Feasibility of Reverberant Shear Wave Elastography for In Vivo Assessment of Skeletal Muscle Viscoelasticity,” in *2020 IEEE International Ultrasonics Symposium (IUS)*, Sep. 2020, pp. 1–4, doi: 10.1109/IUS46767.2020.9251504.
- [31] Y. Zhu *et al.*, “Quantitative analysis of liver fibrosis in rats with shearwave dispersion ultrasound vibrometry: Comparison with dynamic mechanical analysis,” *Medical Engineering & Physics*, vol. 36, no. 11, pp. 1401–1407, Nov. 2014, doi: 10.1016/j.medengphy.2014.04.002.

BIOGRAPHIES OF AUTHORS






Cuong-Thai Nguyen     has a B.E. degree in Information Technology from Hanoi University of Science and Technology in 2004. He also has a Master's degree graduated in Information Technology from Hanoi University of Science and Technology in 2009. Since 2005, he has worked at Hanoi University of Industry, where he is currently a lecturer in the Department of Information Technology. His research interests mainly focus on big data, machine learning, and computer vision. He can be contacted at email: cuongnt@hau.edu.vn.






Pham Thi Thu Ha    is a Master and Technology teacher, Hanoi–Amsterdam High School for the Gifted. She received the master's degree in Cybernetics and Automation Engineering, Military Technical Academy, in 2016. From 2016–2020, she is lecturer, Faculty of Technology Education, Hanoi National University of Education. From 2020 until now, she is technology teacher. The field of scientific interest concerns the modeling and the control of the electric drive systems. Improving energy efficiency and output quality for each system. Desire to apply research results to teaching Technology and STEAM for students. She can be contacted at email: haptt_spkt@hnue.edu.vn.






Pham Duy Phong    is the Dean of the Faculty of Electronics and Telecommunications at the Electric Power University, Hanoi, Vietnam. He received the B.E. degree in Telecommunications Engineering from University of Communications and Transport, Hanoi, in 2000 and the Master degree from Hanoi University of Science and Technology, Hanoi, Vietnam in 2007. He received the Ph.D. degree in the Telecommunications Engineering at Vietnam Research Institute of Electronics, Informatics and Automation, Hanoi, Vietnam in 2013. He was a researcher in Posts and Telecommunications Institute of Technology (2000-2005). His main research interests are radio propagation, antenna design for radio communications, electromagnetic interference on telecommunication systems due to power systems, lightning protection for telecommunication systems. He can be contacted at email: phongphd@epu.edu.vn.






Quang Hai Luong    received a B.E. degree in Electronics Engineering from Le Quy Don Technical University, Vietnam in 2006. He also received an M.S. degree in Control Engineering and Automation from Le Quy Don Technical University in 2013, followed by a Ph.D. degree in Control Engineering and Automation from Le Quy Don Technical University in 2019. Since 2006, he has been working at Le Quy Don Technical. His research interests primarily focus on control engineering and medical image processing. He can be contacted at email: luonghai@mta.edu.vn.



Bao Bo Quoc    received a B.E. degree in Electronics and Telecommunications from the University of Transport and Communications in 2000. He also received an M.S. degree in Information Processing and Communication from Hanoi University of Science and Technology in 2005, followed by a Ph.D. degree in Electrical Engineering from the Institute of Le Quy Don Technical University, Vietnam in 2019. Since 2000, he has been working at Hanoi University of Industry, where he currently holds the position of Vice Dean in the Faculty of Electronics. His research interests primarily focus on signal processing, machine learning, and computer vision. He can be contacted at email: baobq@hau.edu.vn.



Duc-Tan Tran    is a Professor and Vice Dean of Faculty of Electrical and Electronic Engineering (FEEE), Phenikaa University. From August 2016 to May 2019, he was an Associate professor and Vice Dean of Electronics and Telecommunication Faculty, VNU University of Engineering and Technology. He has published over 150 research papers. His publications received the “Best Paper Award” at the 9th International Conference on Multimedia and Ubiquitous Engineering (MUE-15), and International Conference on Green and Human Information Technology (ICGHIT-2015). His main research interests include the representation, processing, analysis, and communication of information embedded in signals and datasets. He can be contacted at email: tan.tranduc@phenikaa-uni.edu.vn.